

RESEARCH ARTICLE

# An empirically grounded agent based model for modeling directs, conflict detection and resolution operations in air traffic management

Christian Bongiorno<sup>1</sup>, Salvatore Micciché<sup>1\*</sup>, Rosario N. Mantegna<sup>1,2</sup>

**1** Dipartimento di Fisica e Chimica, Università degli Studi di Palermo, Viale delle Scienze, Ed. 18, I-90128, Palermo, Italy, **2** Center for Network Science and Department of Economics, Central European University, Nador 9, H-1051, Budapest

\* [salvatore.micciche@unipa.it](mailto:salvatore.micciche@unipa.it)



OPEN ACCESS

**Citation:** Bongiorno C, Micciché S, Mantegna RN (2017) An empirically grounded agent based model for modeling directs, conflict detection and resolution operations in air traffic management. PLoS ONE 12(4): e0175036. <https://doi.org/10.1371/journal.pone.0175036>

**Editor:** Wen-Bo Du, Beihang University, CHINA

**Received:** September 15, 2016

**Accepted:** March 20, 2017

**Published:** April 18, 2017

**Copyright:** © 2017 Bongiorno et al. This is an open access article distributed under the terms of the [Creative Commons Attribution License](https://creativecommons.org/licenses/by/4.0/), which permits unrestricted use, distribution, and reproduction in any medium, provided the original author and source are credited.

**Data Availability Statement:** The research was funded by SESAR-JU (Single European Sky ATM Research joint undertaking) (<http://www.sesarju.eu>) through the research project ELSA “Empirically grounded agent based models for the future ATM scenario”, Contract Number 10-220719-C18. SESAR-JU is a legal entity founded by the European Union and EUROCONTROL (European Organisation for the Safety of Air Navigation), to coordinate and concentrate all relevant research in the technological and operational dimension of the Single European Sky (SES). Data collection was performed by EUROCONTROL. Data were obtained

## Abstract

We present an agent based model of the Air Traffic Management socio-technical complex system aiming at modeling the interactions between aircraft and air traffic controllers at a tactical level. The core of the model is given by the conflict detection and resolution module and by the directs module. Directs are flight shortcuts that are given by air controllers to speed up the passage of an aircraft within a certain airspace and therefore to facilitate airline operations. Conflicts between flight trajectories can occur for two main reasons: either the planning of the flight trajectory was not sufficiently detailed to rule out all potential conflicts or unforeseen events during the flight require modifications of the flight plan that can conflict with other flight trajectories. Our model performs a local conflict detection and resolution procedure. Once a flight trajectory has been made conflict-free, the model searches for possible improvements of the system efficiency by issuing directs. We give an example of model calibration based on real data. We then provide an illustration of the capability of our model in generating scenario simulations able to give insights about the air traffic management system. We show that the calibrated model is able to reproduce the existence of a geographical localization of air traffic controllers’ operations. Finally, we use the model to investigate the relationship between directs and conflict resolutions (i) in the presence of perfect forecast ability of controllers, and (ii) in the presence of some degree of uncertainty in flight trajectory forecast.

## 1 Introduction

According to the majority of predictions the air traffic demand will increase for both business and leisure flights during the next years. This increase will bring the current air traffic management (ATM) system close to its capacity limits. As a consequence an overall improvement of the air transportation system productivity with respect to, for example, traffic flows, air traffic

as part of the SESAR Joint Undertaking WP-E research project ELSA “Empirically grounded agent based model for the future ATM scenario” after competing in a 2011 public call issued by SESAR Joint Undertaking. Anyone interested in the data can request it directly from EUROCONTROL by the following email: [ddr2\\_support@eurocontrol.int](mailto:ddr2_support@eurocontrol.int).

**Funding:** The research was funded by SESAR-JU (Single European Sky ATM Research joint undertaking) (<http://www.sesarju.eu>) through the research project ELSA “Empirically grounded agent based models for the future ATM scenario”, Contract Number 10-220719-C18. SESAR-JU is a legal entity founded by the European Union and EUROCONTROL (European Organisation for the Safety of Air Navigation), to coordinate and concentrate all relevant research in the technological and operational dimension of the Single European Sky (SES). Data collection was performed by EUROCONTROL. Data were obtained as part of the SESAR Joint Undertaking WP-E research project ELSA “Empirically grounded agent based model for the future ATM scenario” after competing in a 2011 public call issued by SESAR Joint Undertaking. Anyone interested in the data can request it directly from EUROCONTROL by the following email: [ddr2\\_support@eurocontrol.int](mailto:ddr2_support@eurocontrol.int).

**Competing interests:** The research was funded by SESAR-JU through the research project ELSA “Empirically grounded agent based models for the future ATM scenario”, Contract Number 10-220719-C18. This does not alter the authors’ adherence to all the PLOS ONE policies on sharing data and materials.

controllers workload and operational efficiency it is urgently needed [1–4]. Within this major change ATM efficiency, safety and resilience standards should be drastically enhanced.

The optimal design of the future ATM system needs a better understanding of the actual air traffic system and of its management procedures. That will be important in order to enhance system’s resilience, safety and capacity. Here we present an agent-based model (ABM) of aircraft and controllers. In our model these agents are acting in an area control center (ACC) of the ATM system. Our model helps understanding the process of the flight trajectory management and it can be used to perform scenario simulations investigating whether modifications of the current operation rules can lead to an improvement in the general efficiency of the ATM system.

Agent-based models started to become popular in the academy and research communities during the early nineties of the last century. During the nineties concepts and tools of complexity, chaos theory, computer science, and cellular automata were incorporated into the wave of development of agent-based modeling [5]. Since these starting years the research field has expanded and evolved developing ABMs within several disciplines and also focusing on topics as calibration and validation of the models [6]. ABMs are consolidated tools in the ATM domain. We can point out three research areas of applications of ABMs. In fact, we have ABMs for the conflict detection and resolution [7], for the management of the traffic flow [8] and for the investigation of the aspects related to the role of human operators [9]. In this work we develop an ABM for conflict detection, conflict resolution and local enhancement of performances of specific flight trajectories.

ABMs for the conflict detection and resolution intervene at a tactical or pre-tactical level and provide methods for detecting and solving (multiple) conflicts on a pairwise or global basis. In Ref. [7] a set of categories has been proposed for the categorization of the different modeling approaches. For example, these categories include the dimensions at which the model works (vertical, horizontal or both), the method of conflict resolution (optimization, brute force, force field, . . .) and the type of maneuvers adopted by aircraft to avoid the conflict (vectoring, flight level changes and velocity changes). The work in Ref. [10] proposed a global method for conflict resolution based on genetic algorithms and taking into account future velocity uncertainties. The conflict detection and resolution algorithm of Ref. [11] is based on a local geometrical resolution of conflicts involving a combination of velocity changes and re-routings. Using the geometric characteristics of aircraft trajectories and intuitive reasoning, closed-form analytical solutions have been developed for optimal heading and/or speed commands. The conflict resolutions are optimal in the sense that they minimize the velocity vector changes required for conflict resolution, resulting in minimum deviations from the planned trajectory. Another approach is the conflict detection and resolution algorithm of Ref. [12]. It is based on a potential field approach that assumes that aircraft are like charged particles interacting in an external electric potential field in its original and simplistic version.

The agents of our ABM are aircraft/pilots and air traffic controllers who are active within an ACC in the European airspace. We simulate flights by tracking how a planned flight plan ends up into a realized one. We are therefore considering the so-called tactical phase of the air traffic management. The basic features of the model have been first introduced in Ref. [13]. A different implementation of the same basic principles has been proposed in Ref. [14, 15].

The model we discuss here is an evolution of the one of Ref. [13]. It consists (i) of a conflict detection module based on the computation of the pairwise distances between all aircraft present in a certain airspace, and (ii) of a module for the pairwise local resolution of conflicts at the tactical level. Our approach is very close in spirit to the one presented in Ref. [11] although their approach rely on a form of numerical optimization. Moreover, our model performs local conflict detection and resolution by using geometrical considerations and by performing

simulations at the level of an ACC. Also it is worth noting that in our model controllers activity is not limited to the resolution of potential safety events. By starting from the consideration that one of the main tasks of controllers is that of facilitating airlines operations we have implemented a module for the issuing of directs in our model. Directs are flight trajectory modifications that are issued by controllers at a tactical level in order to speed up the passage of aircraft within a certain airspace therefore facilitating the airline operations. We believe this is one of the novelties of our model, not present in the models we have recalled above. In our model, once trajectories have been made conflict free the controller searches for possible improvements of the system efficiency by issuing directs. Our implementation of heuristics adopted by controllers to issue directs is based on information about the current state of each specific sector of the airspace as well as on information relative to neighboring airspaces.

Our model can be used to perform scenario simulations able to give insights about the ATM system. For example, our model shows the relationship between the frequency of issued directs and conflict resolution events conditioned to degree of forecasting ability of controllers. This relationship can be relevant to evaluate potentials and problems associated with the evolution of the European ATM system from the current to the so-called SESAR [1] scenario. In fact, due to the foreseen traffic increase, it is expected that the management of the European air transportation system will require major changes to overcome present and future challenges. To tackle these challenges, in 2007 the European Commission created the Single European Sky ATM Research (SESAR) with the scope of coordinating major research and development efforts about air transportation systems performed in Europe. Since then SESAR has been working on defining, exploring, testing, and implementing new solutions to cope with the foreseen air traffic increase. Among these solutions one key concept is that of free-routing [1, 3]. This type of innovation has already been implemented in some limited areas of the European airspace [3]. In fact, in the current scenario, flight plans are given as a sequence of navigation points that have to be crossed at a certain time and at a certain altitude. Navigation points are specific bi-dimensional points of the airspace that are used as a reference in the planning, management and execution of all flights. According to the future SESAR scenario all aircraft will be allowed to plan an optimal trajectory without the constraint of passing through navigation points from departure to arrival. The current scenario, where flight trajectories follow a network of navigation points and pre-defined routes will be progressively abandoned. Currently, air traffic controllers have the role of avoiding conflicts in some specific areas that are mainly located around the navigation points where routes intersect. The implementation of free-routing poses therefore some challenges in terms of safety of the operations and of complexity of the situation that controllers have to manage. For instance, conflicts may become harder to detect due to the fact that they will be spread all over the airspace. Moreover, directs were also used by air traffic controllers as a way to let an aircraft avoid a possible conflict and, at the same time, avoid a conflict. The fact that in the future SESAR scenario all aircraft will follow straight trajectories, will deprive air traffic controllers of such possibility.

A previous version of our model able to perform simulations relevant for the SESAR scenario has been provided in [16, 17]. The present version of the model expands the possibilities of simulations useful to evaluate robustness and performances of different implementations of the SESAR scenario and of any other scenario of evolution of the air transportation system.

The paper is organized as follows. In section 2 we present the data used for the empirical characterization of the system and for model calibration. In section 3 we describe the main features of the modules of the ABM. In section 4 we summarize the model calibration. In section 5 we show a few results obtained with our ABM using the model parameters obtained with the calibration procedure and in section 6 we show a few results obtained with our ABM and trying to exploit the possible range of model parameters. In section 7 we finally draw our conclusions.

## 2 Data

Original data are collected by Eurocontrol, the European public institution that coordinates and plans air traffic control for all Europe. Data were obtained as part of the *SESAR Joint Undertaking* WP-E research project ELSA “Empirically grounded agent based model for the future ATM scenario”. Data can be accessed by asking permission to the owner (Eurocontrol). Eurocontrol databases include all flights occurring in the enlarged European Civil Aviation Conference (ECAC) airspace even if they departed and/or landed in airports external to the enlarged ECAC airspace. Countries in the enlarged ECAC space are: Iceland (BI), Kosovo (BK), Belgium (EB), Germany-civil (ED), Estonia (EE), Finland (EF), UK (EG), Netherlands (EH), Ireland (EI), Denmark (EK), Luxembourg (EL), Norway (EN), Poland (EP), Sweden (ES), Germany-military (ET), Latvia (EV), Lithuania (EY), Albania (LA), Bulgaria (LB), Cyprus (LC), Croatia (LD), Spain (LE), France (LF), Greece (LG), Hungary (LH), Italy (LI), Slovenia (LJ), Czech Republic (LK), Malta (LM), Monaco (LN), Austria (LO), Portugal (LP), Bosnia-Herzegovina (LQ), Romania (LR), Switzerland (LS), Turkey (LT), Moldova (LU), Macedonia (LW), Gibraltar (LX), Serbia-Montenegro (LY), Slovakia (LZ), Armenia (UD), Georgia (UG), Ukraine (UK).

Original data are recorded in the demand data repository (DDR) files where information consists of the trajectories of flights, along with some additional information about flights (IATA code, type of aircraft, among the others). The other source of information is given by the network estimation visualization of ACC capacity (NEVAC) files. NEVAC files [18] contain the definition (borders, altitude, relationships, time of opening and closing) of airspace elements, namely airblocks, sectors, Flight Information Region (FIR), etc. The active elements, at a given time, constitute the configuration of the airspace at that time. Thus, they give the configuration of the airspaces for an entire AIRAC cycle. In the present study we only use the information on sectors, FIRs or ACCs and configurations to rebuild the European airspace.

To properly process this large amount of structured data. We have populated a specialized database using selected records of DDR and NEVAC original files. The structure and the type of data retained in this specialized database have been described in Ref. [19]. In the present paper, we analyze data referring to the Aeronautical Information Regulation and Control (AIRAC) cycle beginning on May 6th, 2010 and ending on June 3rd, 2010, corresponding to the AIRAC cycle number 334. We use the information of the DDR files in order to set some filters. In fact, from the database we remove a certain number of flights that are not directly related to commercial air traffic management. For example we remove military flights in operation. Hereafter we list the filters we used to select our set of data: (a) all flights occurring during weekdays; (b) flights having at least two points in the Italian ACC airspace (LIRR); (c) flights with at least two navigation points crossed at an altitude higher than 240FL in the flight plan; (d) only non-military and commercial flights having a IATA code; (e) only land-plane aircraft, i.e. no helicopter, gyrocopter, etc; (f) flights with a duration longer than 10 minutes.

A planned or a realized trajectory is made by a sequence of navigation points planned or crossed by the aircraft, together with altitudes and timestamps. For each flight, we have access to two different flight plans: the last filled plan (labeled as M1 type file)—filed from 6 months to one or two hours before the real departure—and the realized flight plan (labeled as M3 type file), describing the real trajectory updated by radar tracks. Our study investigates air traffic management on the en-route phase. After the filtering procedure 35704 flights are retained in the investigated AIRAC. In order to include the local constraints of the sector capacities, sectors are defined as described in reference [20]. These sectors are static bi-dimensional projection of the sectors higher than FL 350.

### 3 The model

In our agent-based model we have two types of agents: (i) aircraft/pilots that are active within an ACC of the European airspace, and (ii) air traffic controllers (ATCOs) that manage the flight trajectories in the different sectors of the ACC. The pilots are passive agents, in fact they follow the flight plan or the instructions of the ATCOs if they were different. The ATCOs monitor the execution of the flight plan. The type of actions decided by controllers depends by the current workload of their own sector and by the workload of the neighboring sectors as well as by the details of the flight plans. Our ABM simulates realizations of the en-route phase of the flight trajectories originally planned.

The interaction between the aircraft/pilots and air traffic controllers is needed in order to manage the changes from the planned flight due to unforeseen events, e.g. weather events, conflict resolutions, etc. Another important task involves the issuing of directs. A direct is a change of trajectory from the planned one such that the aircraft is allowed to follow a shorter flight trajectory by skipping one or more navigation points of the M1 flight-plan. In fact, whenever possible, the model allows directs that are given within an ACC in order to speed up the passage of the aircraft, provided that no additional conflict is created.

#### 3.1 Overview of the model

A schematic block diagram of the model is given in Fig 1. The logical blocks shown in the left part of the figure are described in sections 3.3 and 3.4. They are relative to the set up of aircraft trajectories and sector configuration. In these modules the model computes the position of the aircraft with a certain look-ahead, estimates the sectors workload and defines the pairs of aircraft to be verified the one against the other in order to check for possible conflicts. The logical blocks shown in the right part of the figure are described in sections 3.5 and 3.7. They refer to the en-route management of flight trajectories needed either to solve possible conflicts or to issue directs in order to shorten the passage of an aircraft in a sector. In section 3.5 we describe (i) how distances between aircraft pairs are computed within the model, (ii) how this information is used in order to identify the aircraft pairs that are below a safety threshold and (iii) how trajectories are modified in order to solve the conflicts. Finally, in section 3.7 we describe how directs are issued, after checking that safety requirements and capacity constraints are not infringed.

We have designed the code in a modular way that allows to swap the priority of the strategies adopted by the controllers. In fact, as a default controllers first check for the possibility of doing re-routings and then change the flight altitude (FL change). Therefore, due to the modularity of the code, the sequence among the different modules can be changed by the user of the code.

The code that implements the present model is written in C [21] and it is available at the following URL: <http://ocs.unipa.it/software.html:ELSATacticalLayer>. A previous version of the code specifically dedicated for performing simulations in the SESAR scenario is available at the following URL: <http://ocs.unipa.it/software.html:ELSASESARSimulator>.

#### 3.2 Navigation points

The planned flight trajectories are sequences of specific points of the airspace called navigation points that are crossed by the aircraft at specific times, flight levels, and within a specific sector. The velocity of each aircraft during the flight interval between two navigation points is assumed to be constant and its value is estimated from the schedule of the flight plan. In our simulations all navigation points present in the last-filed flight-plans are used. When controllers decide a flight trajectory change they might use temporary navigation points that are set by the ABM model in a way similar to what is done by controllers in real cases documented in

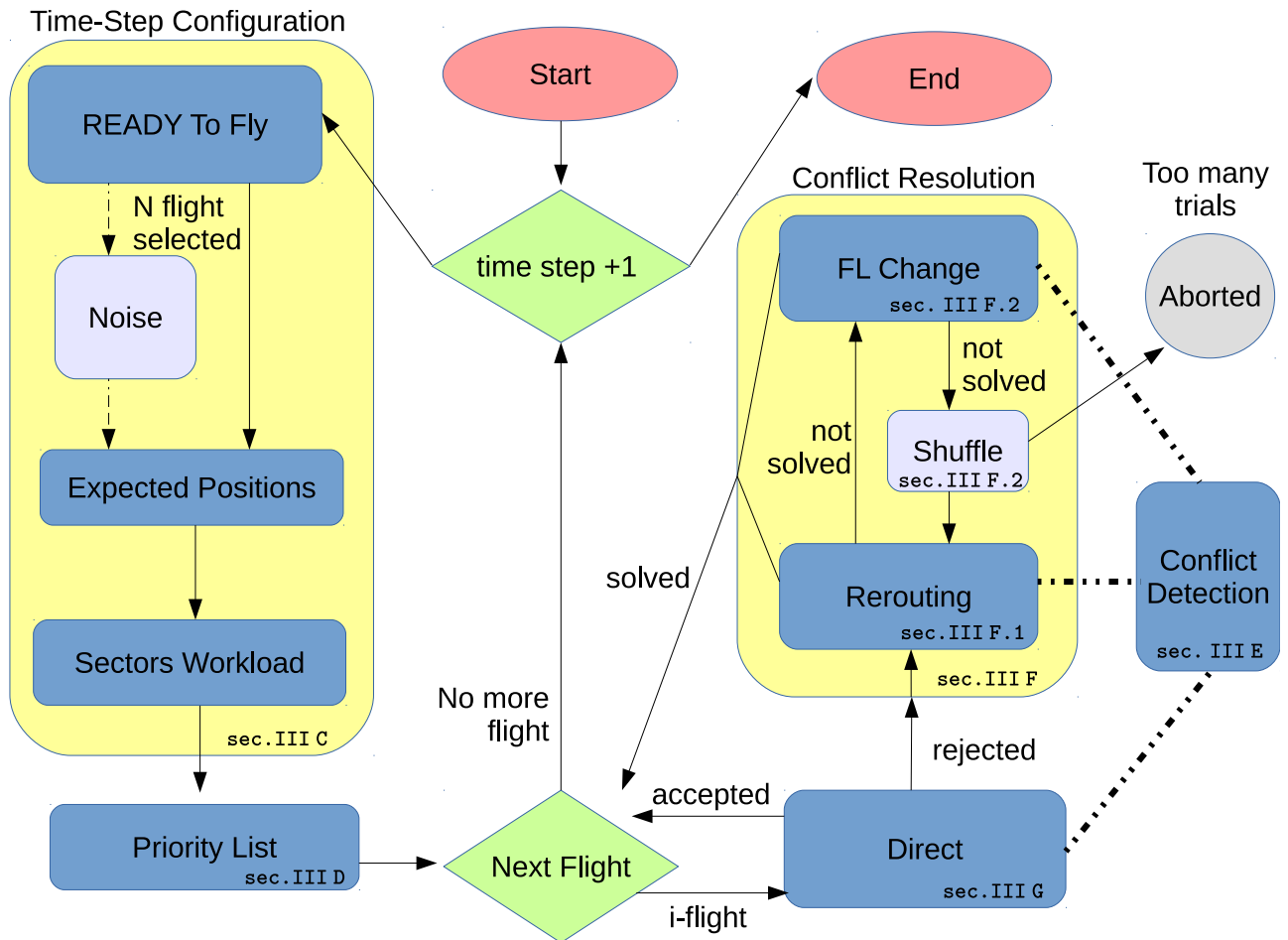


**Fig 1. Schematic block diagram of the tactical ABM model.** Red blocks identify the start and the end of the code. Rectangular cyan boxes indicate the different modules of the model where operational steps are performed. Larger rectangular yellow areas are used to identify different large modules of the model: the one on the left is devoted to the set up of aircraft trajectories and sector configuration and the one on the right is devoted to the management of flight trajectories. Green blocks identify the logical nodes where choices are done. Arrows are indicating directed connections of different blocks. Dashed lines highlight the fact that a module is interacting with the *Conflict Detection* module. For several blocks we indicate the section where the block is described.

<https://doi.org/10.1371/journal.pone.0175036.g001>

the historical data we use. In the simulations we present in this paper the temporary navigation points are randomly uniformly distributed within the Italian ACC.

It should be noted that not all temporary navigation points will be used in the flight deviations. Only a set of them will be selected, as we will explain below. All the unused ones will be eliminated from the analysis after all the flights in the ACC will be managed. As we will explain in section 3.6.1, they are generated to allow the aircraft to deviate from the planned trajectories without necessarily passing over a predefined navigation point which might be too far.

### 3.3 Time-step configuration

The ABM is a discrete-time model. At each time-step the *ReadyToFly* module selects the active aircraft, then the *Expected Position* module computes the expected dynamical evolution of all trajectories within a look-ahead  $\Delta t$ . In fact, we have two possible look-ahead  $\Delta t$ , that are used depending on the controllers' activity. The look-ahead assumes the value  $\Delta t = \Delta t_d$  when the

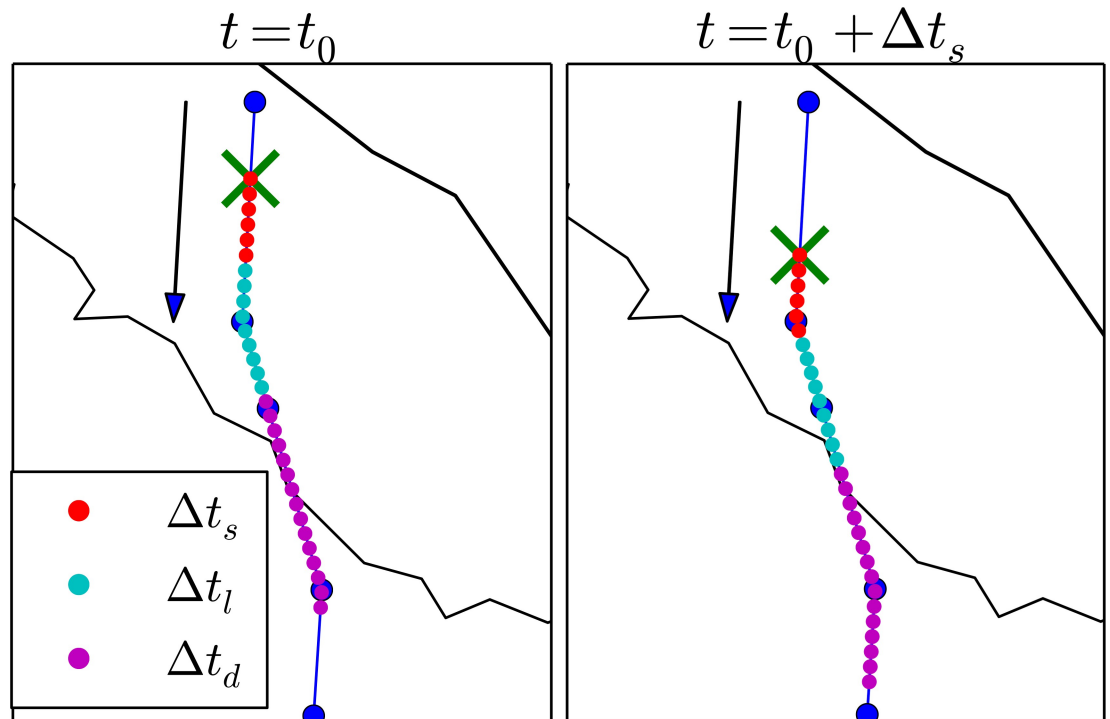


**Fig 2. Illustration of the time discretization used in the model.** In the two panels we show a flight trajectory sampled at discrete times with an elementary time interval of  $\delta t = 30$  sec. The dots indicate the aircraft positions sampled at each  $\delta t$ . Red dots are the aircraft positions evaluated within a time step  $\Delta t_s = 3$  min for the flight trajectory evaluated at  $t = t_0$  (left panel) and at  $t = t_0 + \Delta t_s$  (right panel). Red and cyan dots are the aircraft positions evaluated within the time interval of the look-ahead  $\Delta t_l = 7.5$  min whereas red, cyan and magenta dots are the aircraft positions evaluated within the time interval of the look-ahead used to issue directs  $\Delta t_d = 15$  min. Blue circles are navigation points of the flight plan. The cross indicates the initial aircraft position at the initial time of the time step. The arrows indicate the directions travelled by the aircraft.

<https://doi.org/10.1371/journal.pone.0175036.g002>

ATCO checks the trajectories for possible safety issues during the preliminary procedures necessary before taking the decision of issuing a direct (see section 3.7 for a detailed description of these procedures). The look-ahead assumes a smaller value  $\Delta t = \Delta t_l$  when the ATCO performs only the checks for conflict detection.

At time  $t_0$  let us suppose that the position of all aircraft is known. The elementary time step of the model is  $\delta t$ . In our model  $\Delta t_d$  and  $\Delta t_l$  are integer multiple of  $\delta t$ . At time  $t$  the time evolution of the system is computed with  $\delta t$  time resolution until the time  $t + \Delta t$  where  $\Delta t$  is the look-ahead time of air traffic controllers. On the basis of the estimated time evolution air traffic controllers release their decisions to the aircraft and a new iteration starts. To minimize the computational cost of the simulation the initial time of the next model iteration is performed at time  $t + \Delta t_s$  where  $\Delta t_s$  is a time interval ranging between  $\delta t$  and  $\Delta t$ . The values used in our simulations after calibration were  $\delta t = 10$  seconds,  $\Delta t_l = 7.5$  minutes,  $\Delta t_s = 3$  minutes and  $\Delta t_d = 15$  minutes, see Fig 2.

Indeed, in the basic setup, the controller forecast of the aircraft position is exact within its time look-ahead. Our ABM allows to introduce some errors in the forecast of the controller. This is done by setting a parameter  $l_\epsilon \neq 0$  which is controlling the uncertainty in the estimation of the velocity of the aircraft. Specifically, the uncertainty in the controller's forecast is introduced by the following procedure: (i) between time  $t$  (current time) and  $t + \Delta t_s$ , each aircraft maintains the planned velocity, (ii) between  $t + \Delta t_s$  and  $t + \Delta t_d$ , the model introduces an

uncertainty in the aircraft velocity. The velocity used by the controller is  $v(1 + \epsilon_v)$ , where  $\epsilon_v$  is drawn at random from a uniform distribution in the range  $-l_\epsilon$  and  $l_\epsilon$ . With this choice the controller makes bigger errors on positions on longer times. The choice of considering a uniform distribution is done for the sake of simplicity. That gives us the opportunity of exploring the impact of uncertainty in the ATCOs management procedures. Hereafter, we will consider two rather different cases:  $l_\epsilon = 0$  (no uncertainty) and  $l_\epsilon = 0.1$  (10% of maximal uncertainty).

The velocity of aircraft is always the one of the planned flight trajectories in the time interval between  $t$  and  $t + \Delta t_s$ . The only possible exception is in the case of re-routings, as explained below. The *Sectors workload* module is used to set up the configuration of airspace sectors and to determine the number of aircraft present in each sector analyzed by ATCOs. In fact, any ACC is divided into a number of sectors. Each sector is characterized by its geographical boundaries and its capacity. Usually such capacity is set in advance by the service providers. Since we do not have such information, we infer the capacity from data and we estimate it as the maximum number of aircraft that are simultaneously present in a sector within a time window of one hour [20]. This information is obtained from the flight plans of the AIRAC used in our simulations. In addition to the inferred capacity of a sector, we also dynamically estimate its workload. Specifically, we estimate a sector workload as the number of flights planned to cross the sector during the time window of an hour. At each time-step the ABM evaluates the workload of each sector of the ACC.

### 3.4 Priority list of controllers' actions

At each time step we create a list of flights active in the considered time-step. The list is randomly ordered. The order of the list is followed by the controller in her attempt to solve potential conflicts and to issue directs. Specifically, the  $i$ -th aircraft trajectory in the list is checked against the trajectories of previous listed  $i - 1$  flights. For example, the first aircraft in the list will perform its planned trajectory whereas the trajectory of the second one will be checked with respect to the trajectory of the first one. The trajectory of the third aircraft will be checked with respect to the trajectories of the second and the first ones and so on. Indeed, to speed computation, the trajectory check between two aircraft is not performed when the two trajectories are too far to interact within the look-ahead time interval.

The random reordering of the flight priority list is done in order to be sure that the trajectories to be deviated are not always the same ones. If a conflict involving the  $i - th$  aircraft is not solved by one of the procedures followed by the controller, then the list is modified by putting the  $i - th$  aircraft in the first position of the list and the trajectory analysis of the time step is repeated from the beginning. When this redefinition of the priority list is repeated more than 50 times for a time step the simulation is aborted. It is worth reporting that we never had to abort a simulation in the runs performed to obtain the results presented in this paper.

### 3.5 Conflict detection module

The collision detection module calculates the minimum distance for each pair of aircraft positions between the flight  $i$  and the flights labeled as  $i - 1$  in the priority list. This operation is repeated for all the times  $t + k\delta t$  with  $k$  ranging from 1 to  $N$  such that  $t + N\delta t \equiv t + \Delta t_m$  where  $\Delta t_m$  is equal to  $\Delta t_t$  or  $\Delta t_d$  depending whether the conflict detection module has been activated by a re-routing procedure or by a direct procedure. For each flight  $i$  the algorithm computes an array of flight positions  $p_{i,k}$ ,  $k = 1, \dots, N$  given the flight positions at different time  $t + k\delta t$ .

Suppose we are now checking if the  $i$ -th flight trajectory is conflicting with all other  $f_j$  trajectories, with  $j < i$ . For each of the  $N$  elementary time-increments, we compute a matrix of distances  $d_{j,k}^i$  with  $j$  rows and  $N$  columns. For all aircraft flying at the same flight level all distances



are computed by using the Haversine distance [22] between each pair of flight positions. It is worth mentioning that the computation of the Haversine distance is particularly time-consuming. Therefore we have also implemented in the code the possibility that in some specific cases the Euclidean distance is used instead of the Haversine one. This is for example advised when it is necessary to perform a very large number of simulations in a limited portion of the airspace.

For pairs of aircraft flying at different flight levels at time  $t + k\delta t$  the distance is set to infinity because aircraft flying at different flight level are not raising minimum separation issues. For each column we select the minimum value and obtain a vector  $d_{min}^i(k)$  of length  $N$ . A possible conflict between two aircraft flying at the same flight level is detected at time  $t + k\delta t$  whenever the elements of  $d_{min}^i(k)$  are smaller than the safety distance threshold  $d_{thr}$  that is usually set to 5 NM. This reference value is the standard value used in ATM for conflict detection, see Ref. [23].

In order to mimic some heuristics typically used by air traffic controllers when detecting conflicts we introduce in the ABM a linear growth of the safety threshold  $d_{thr}$  as a function of the time interval from the present time. In fact when an air traffic controller forecasts the position of an aircraft at a far future time he uses an additional space of separation between the aircraft to be safe in the forecast. Our model therefore uses a safety distance threshold defined as:

$$d_{thr}(k) = d_{thr} + \Delta d_{thr}k \tag{1}$$

where  $\Delta d_{thr}$  is one of the model parameters.

When a conflict is detected the algorithm proceeds to the next module that performs the de-conflicting of flight trajectories.

### 3.6 Conflict resolution module

After the conflict detection module has detected a conflict, this module searches for a new conflict free trajectory. It is conceived as a two-step algorithm that acts on the search of a new trajectory. The first step attempts to perform a re-routing of the flight trajectory. When the re-routing is successful the new trajectory is accepted. If the re-routing module fails to find an appropriate new trajectory the algorithm moves to the second step that requires a change of flight level for the aircraft.

**3.6.1 Re-rerouting submodule.** The procedure of the re-routing attempt is illustrated in Fig 3. We first identify the position  $B$  (not necessarily a navigation point) defined by  $k = 0$  at the considered time step. We then identify the navigation point  $A$  which is the first navigation point after the area of the potential collision (filled circle in the figure). With such procedure we are attempting to re-route the trajectory so that all navigation points that are in the conflict area plus the  $A$  navigation point are avoided. These navigation points are replaced by one temporary navigation point (see  $T$  point in Fig 3). The temporary navigation point is selected from several possibilities (see grey points in Fig 3) by choosing the navigation point solving the conflict that presents the shortest path between position  $B$  and navigation point  $E$ , i.e. the navigation point where the flight trajectory is re-routed. Another constraint about the re-routing trajectory is the request that the deviated trajectory from the planned one cannot exceed an angle  $\alpha_M$  both for the  $\alpha_{in}$  and  $\alpha_{out}$  angles observed between the planned and the re-routed trajectories (see Fig 3). We set the average velocity of the aircraft in the new trajectory segments equal to the average velocity of the replaced planned trajectory segments.

If the re-routing trajectory is not able to find a solution the re-routing submodule attempts to re-route the flight trajectory by moving forward the navigation point  $E$  and by looking again for a re-routing trajectory. When a possible solution is found, the result of the search is

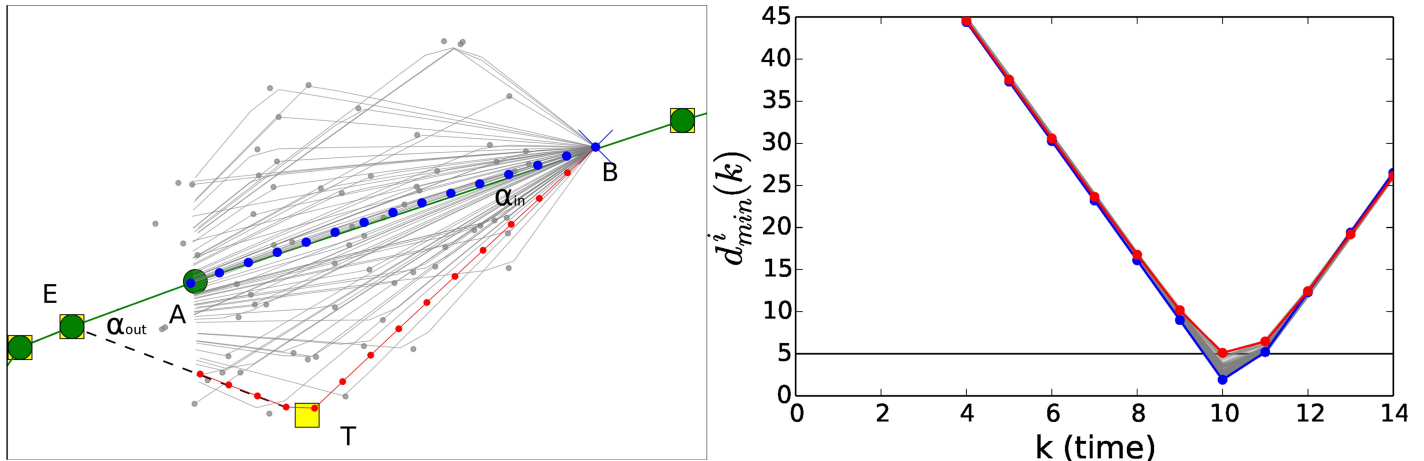


**Fig 3. The figure illustrates the procedure of re-routing, see text for more details.** The gray trajectories, although possible, are not selected because they do not guarantee the minimum separation of 5 NM required between two aircraft. The re-routing occurs between point B (blue cross of the left panel) and E (green circle of the left panel). The re-routing is performed by deviating the flight trajectory to the temporary navigation point T (yellow square of the left panel) and then re-route back the trajectory to navigation point E. To find the best re-routing flight trajectory the ABM module explores trajectories passing through several different temporary navigation points (gray spots of the left panel). The distance between the two aircraft is shown in the right panel for the planned trajectory (blue dots), the ones considered by the ABM module (gray lines) and the selected one satisfying the requirement of minimum separation distance (red dots). In the left panel all trajectories are considered within the time of the look-ahead  $\Delta t_i$ .

<https://doi.org/10.1371/journal.pone.0175036.g003>

accepted if the re-routing trajectory deviates from the planned trajectory for less than a maximal time  $T_{max}$ .  $T_{max}$  is the maximal time that an aircraft can spend away from its planned trajectory each time its flight trajectory is modified. If the solution found has a deviation time longer than  $T_{max}$  the re-routing submodule is not selecting any new trajectory and the resolution of the conflict is passed to the flight level module. In the right panel we show the distance between the two aircraft for the planned trajectory (blue dots) and the ones considered by the ABM module (gray lines). Amongst those, the trajectory that satisfies the requirement of minimum separation distance is highlighted in red, as in the left panel.

**3.6.2 Flight level change submodule.** The second step of the conflict resolution module involves changes of flight level. A flight level (FL) is a unit measure defined as altitude above sea-level in 100 feet units measured according to a standard atmosphere. Allowed flight levels are separated by 1000 feet, i.e. 10 flight levels (separation levels). This is the standard separation vertical distance between any pair of aircraft, see Ref. [23]. Moreover, in our model the semi-circular rule has been considered, meaning that aircraft flying in opposite directions are allowed to fly only along odd or even levels respectively. Therefore when an aircraft needs to be moved to another separation level, it will not be moved to the next first one but to the second one in order to respect the semicircular rule, thus performing a jump of 2000 feet or 20 FLs.

All flights are considered to be available in the planned trajectories. In our agent based model aircraft can move two Flight Levels (FL) first upwards and, if the conflict cannot be solved by a move upwards, downwards. The model assumes that the flight level change is abrupt occurring when the conflict resolution is settled. If no flight level is available to solve the conflict then the list is reshuffled by moving the considered flight in the first position of the priority list.

When a flight level change is executed the flight remains in the new flight level for a time equals to  $T_{max}$ . After  $T_{max}$  the aircraft goes back to the flight level of the planned flight.

### 3.7 Direct module

A direct, i.e. a change of the planned trajectory significantly shortening the flight path, is made by skipping one or more navigation points of the flight plan and flying straightly from the current navigation point to a distant navigation point of the flight plan. In our algorithm this module is executed with a probability depending on the workload of sectors of initial and ending navigation points of the direct.

When the monitored workload of a sector exceeds its inferred capacity all requests of directs that come from other sectors are not allowed while re-routing due to safety issues are still allowed. This means that, no change with respect to the planned trajectories is allowed when the workload equals or exceeds the inferred capacity with the exception of those changes triggered by the need of a resolution of a safety event. Under this workload condition incoming flights have to enter the sector through the navigation point specified in the original flight plan.

Specifically, let  $n_i$  be the first navigation point to be crossed of the current time step, and  $n_m$  the navigation point where the flight will return on its original flight plan. By issuing a direct trajectory from  $n_i$  to  $n_m$  therefore  $m - i - 1$  navigation points will be eliminated from the new trajectory, as illustrated in the left panel of Fig 4.

The direct module first evaluates how many navigation points can be skipped with the constraint that the flight has to come back to the planned trajectory within a time interval equal to  $T_{max} = 20$  min, and the direct is conditioned to the inferred sectors' capacity of the adjacent sectors. Such choice of  $T_{max}$  has been done in agreement with the indications of the air traffic controllers consulted within the ELSA project of SESAR.

Successively, the model evaluates if the new trajectory will be involved in conflicts. In order to do this check we use the Conflict Detection module of section 3.5 where we set the look-ahead  $\Delta t = \Delta t_d$ . If the direct is safe and the angle between the new and original trajectory is larger than a sensitivity threshold value  $\alpha_s = 1^\circ$  then the new trajectory is accepted, otherwise the algorithm tries a suboptimal solution, see the left panel of Fig 4.

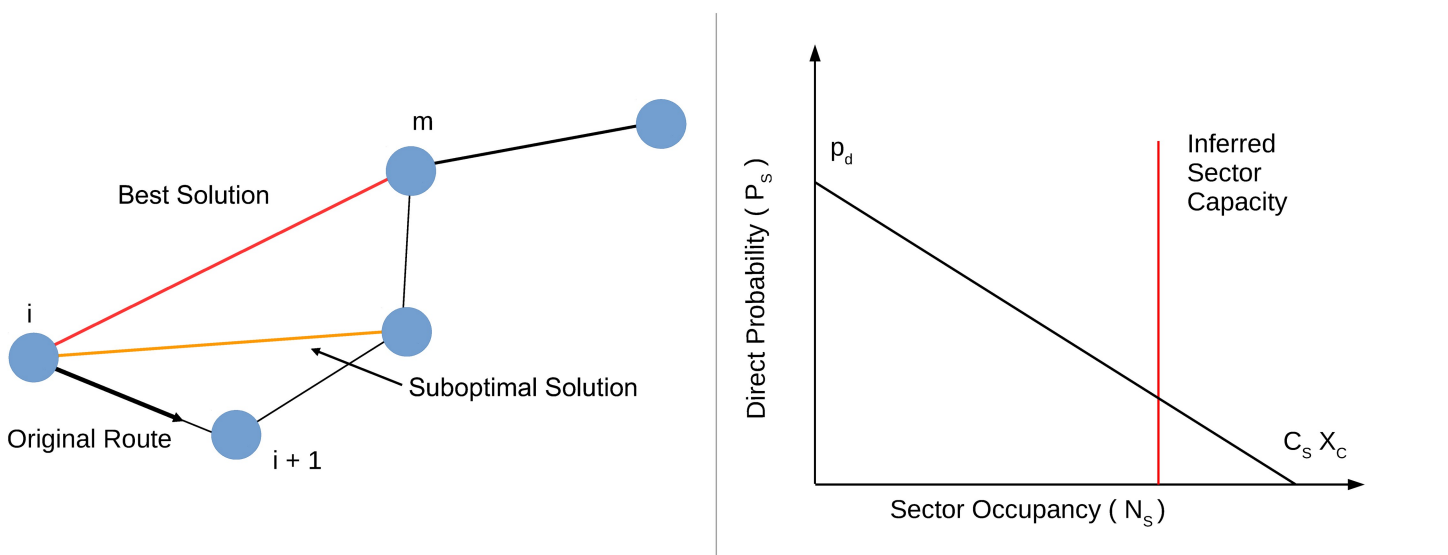


**Fig 4.** Left panel: illustration of the procedure implemented to issuing directs. Right panel: Probability function used in the procedure implemented to issuing directs.

<https://doi.org/10.1371/journal.pone.0175036.g004>

The probability to issue a direct for an ATCO operation on a sector  $s$  is dependent on the workload and by the inferred capacity of the considered sector. Let  $C_s$  be a constant of the  $s$ -sector that in our calibration procedure we fixed to be the inferred sector capacity obtained from real data [20]. Let  $P_s(N_s)$  be the probability to issue a direct in the  $s$ -sector when the workload of sector  $s$  is  $N_s$ . For the sake of simplicity we model  $P_s(N_s)$  as a linear decreasing function of  $N_s$ , see the right panel of Fig 4,

$$P_s(N_s) = p_d \left( 1 - \frac{N_s}{x_c C_s} \right). \tag{2}$$

The probability to attempt a direct is function of two parameters  $p_d$  and  $x_c$ . The first  $P_s(N_s = 1) = p_d$  is the probability to attempt a direct if just one flight is in the sector. The second parameter  $x_c$  is used to control the slope of probability as a function of the workload, as illustrated in the right panel of Fig 4. The  $p_d$  parameter plays the role of a scale factor for the overall probability. The  $x_c$  parameter measures the controllers confidence in approaching the maximum sector's inferred capacity. While  $N_s$  and  $C_s$  are parameters depending on each specific sector,  $p_d$  and  $x_c$  are global parameters that are set across the whole considered ACC.

In the present version of the model, air traffic controllers behave in the same way in the different sectors. However, by introducing a direct probability  $P_s$  that depends on the actual inferred capacity of each sector, see Eq 2, we have realized a genuinely multi-sector ABM where directs are issued differently across the ACC and across the day. The choice of the use of the same parameters for different controllers and sectors (except inferred capacity) is done in order to make the ABM model as parsimonious as possible.

### 3.8 Model's parameters

In Table 1 we summarize the model's parameters used in the different modules described above. In the third column of the Table we give a short description of the parameter and in the fourth column we give a categorization of the parameters describing whether the parameter is calibrated from data (CD) or it is set according to information obtained by interviewing ATM experts and ATCOs (CV).

The parameters that need to be calibrated from data are a few. There are also several parameters (CV category) that can be inferred from the typical behavior of controllers. These are

**Table 1. Model parameters.**

ID	Parameter	Description	Type	Value
1	$\delta t$	Length of the elementary time-interval.		10 s
2	$\Delta t_f$	Length of the forecast for collision, controller's look-ahead.	CD	7.5 m
3	$\Delta t_d$	Length of the forecast for directs.	CV	15 m
4	$\Delta t_s$	Basic time step.		3 min.
5	$l_\epsilon$	Aircraft velocity noise range		0; 0.1
6	$d_{thr}$	Safety Distance threshold.	CV	5NM
7	$\Delta d_{thr}$	Increment of the safety distance threshold in the forecast.	CV	0; 0.33 in section 5.1
8	$\alpha_M$	Maximum angle of deviation between planned and re-routed trajectory.	CV	27 deg.
9	$T_{max}$	Maximum time spent outside the planned flight trajectory.	CV	20 min.
10	$p_d$	Unconditional probability to try to issue a direct.	CD	0.24
11	$x_c$	Tolerance to the sector congestion.	CD	0.63
12	$\alpha_s$	Minimal angle to issue a direct.		1°
13	$C_s$	Sector inferred capacity.	CD	Sector's specific

<https://doi.org/10.1371/journal.pone.0175036.t001>

parameters that should be selected by consulting ATM experts and ATCOs. It is worth noting that by considering these variables as parameters our model allows to perform scenario simulations to test how changing a certain feature of air traffic controllers might affect ATM performances.

## 4 Calibration of the model

In this section we want to discuss the calibration activities that have to be performed in order to use our model.

We will here refer to the air-traffic of LIRR ACC (Rome, Italy) between 2010-05-06 and 2010-06-03, i.e. the 334 AIRAC. The input data of the model are taken from the database developed within the ELSA [24, 25] project and briefly described in section 2. We consider as an input to the model the M1 flight plans with the constraints indicated in section 2. To focus our attention on the en-route phase we filtered out from the flight plans all navigation points crossed at an altitude lower than 240FL. After the filtering procedure 35704 flights were retained in the entire AIRAC. In order to include the local constraints of the sector capacities, it is important to remember that the sectors are not static geometric regions but they are merged together and split dynamically to fulfill the occupancy requirement. For the sake of simplicity we will refer to the collapsed sector defined in the reference [20]. These are a static bi-dimensional projection of the sectors higher than FL 350. The sectors capacity inferred from data is defined as the maximum number of flight expected within a time-window of one hour inside the collapsed sector.

In this section we describe our calibration procedure. In our simulations we consider the scheduled flights of the LIRR ACC (Rome, Italy) of the AIRAC 334 described in section 2. The calibration procedure is performed by choosing a specific stylized fact observed in real data and requesting that model simulations are able to reproduce them.

Indeed, there is some degree of arbitrariness in selecting the specific stylized fact. Different ones can be chosen depending on the specific aspects of the ATM researchers want to investigate. In the present work, in order to calibrate the models parameters related to controllers' behavior we choose as stylized fact a statistical regularity concerning the intraday pattern of directs issued by ATCOs. Specifically we calibrate our model to reproduce the intraday evolution of the deviation rate metric that has been recently introduced in Ref. [26].

The deviation rate introduced in Ref. [26] quantifies the deviations observed from the planned flight trajectories. We call *deviation* the event such that an aircraft passing over a scheduled navigation point does not go to the next planned one. The deviation rate is defined as the ratio between the observed number of deviations and the number of possible deviations in the airspace estimated in a one hour time window. The number of possible deviations is defined as the number of planned navigation points that are actually crossed by the aircraft. This metric is computed for each hour of the day by using the information about all planned and realized flight trajectories.

This metric describes an unknown mixture of ATCO operations, i.e. re-routing and direct. In [26] it is shown that, in relative terms, directs are mainly issued during night-time i.e. in low traffic conditions while they are relatively less issued during day-time. Our choice is to reproduce this intraday statistical regularity. In the right panel of Fig 5 we show (blue circles) the empirical behavior of the deviation rate estimated over the entire 334 AIRAC cycle as a function of the time of the day. The deviation rate presents a U-shape having higher values during night hours and lower values during day hours. The error bars are computed as the 95% Wilson score interval [27] used to associate a confidence interval to a proportion in a statistical population.

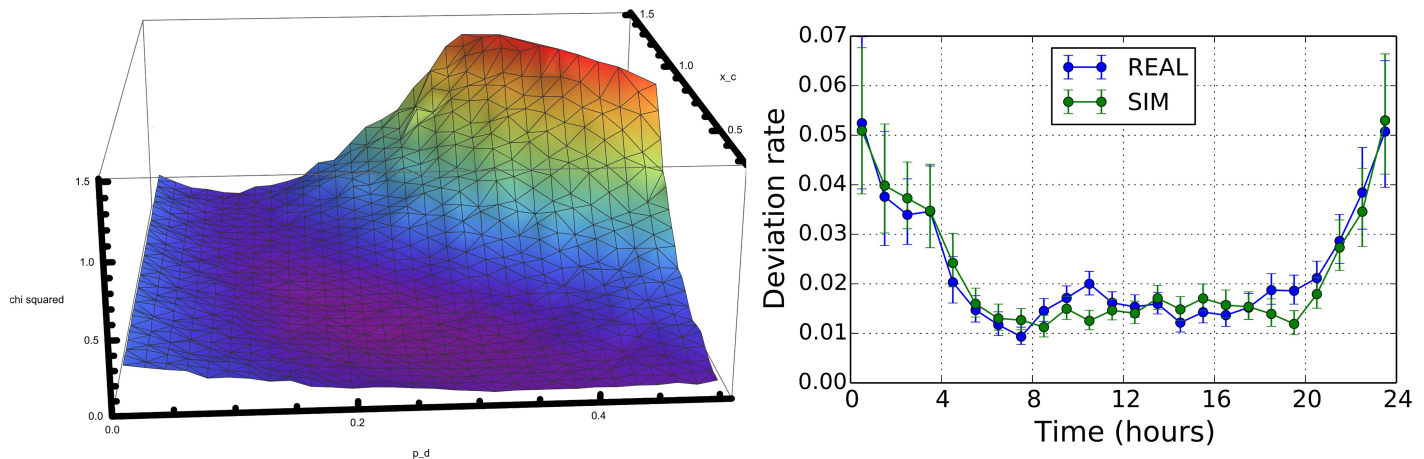


**Fig 5. Illustration of the calibration procedure.** Left Panel: we are showing the values of the  $\chi^2$ , as a function of  $p_d$  and  $x_c$  when  $\Delta t_l = 7.5$  minutes. Right Panel: we show the empirical (blue circles) behavior of the deviation rate metric averaged over the entire 334 AIRAC cycle. The solid green line shows the deviation rate metric obtained by performing a simulation of the model with the selected parameters  $p_d = 0.2465$  and  $x_c = 0.6310$  and  $\Delta t_l = 7.5$  min.

<https://doi.org/10.1371/journal.pone.0175036.g005>

Hereafter we detail the procedure we have used to calibrate  $p_d$ ,  $x_c$  and  $\Delta t_l$  parameters. In our calibration procedure we considered  $p_d \in [0.03, 0.5]$  with steps of 0.01567,  $x_c \in [0.34, 1.5]$  with step of 0.03867 and  $\Delta t_l \in [5, 15]$  minutes with steps of 2.5 minutes and for each triplet of parameters we performed one single simulation for each considered day in the AIRAC, totaling 20 days of simulations—with Saturday and Sundays excluded. From the output of the ABM we estimated the deviation rate with a time window of one hour. By using the results of simulations, we minimized the chi-squared  $\chi^2$  computed starting from the deviation rates obtained with the ABM and the values estimated from real data. The  $\chi^2$  is therefore computed over 24 points. In the left panel of Fig 5 we are showing the average values of the  $\chi^2$ , as a function of  $p_d$  and  $x_c$  when  $\Delta t_l = 7.5$  minutes. The lowest value of  $\chi^2$  is associated to  $p_d = 0.2465$  and  $x_c = 0.6310$  and  $\Delta t_l = 7.5$  min. This set of parameters corresponds to  $\chi^2 = 0.01294$ . However, it is worth noticing that a larger region of parameters (see the magenta region) could still provide acceptable set of parameters. The solid green line in the right panel of Fig 5 shows the deviation rate metric obtained by performing the simulation of the model with the selected parameters  $p_d = 0.2465$  and  $x_c = 0.6310$  and  $\Delta t_l = 7.5$  min.

Here we want to assess the importance of the calibration procedure. In fact, in Fig 6 we show results that can be obtained by our model by choosing sets of parameters different from the calibrated ones. The first example sets that no direct is issued (left panel of Fig 6). The “No Directs” case is obtained by setting  $p_d = 0$  and  $\Delta t_l = 7.5$  min. The second example sets that the probability to issue a direct is independent from the sector workload (right panel of Fig 6). This second example is obtained by setting to the case when  $p_d = 0.24$ ,  $\Delta t_l = 7.5$ , as in the calibrated case and  $x_c = 1000$ . Such a value of  $x_c$  ensures that the sector workload plays no role when directs are issued. With the chosen parameters we have that the deviations rate simulated during night-time corresponds to the empirical case.

## 5 Statistical regularities of ABM simulations

In this section we give some examples of the simulation outputs of our model obtained with the parameters of the calibration procedure of section 4 for the evolution of the planned flight trajectories of the LIRR ACC (Rome, Italy) of the AIRAC 334.

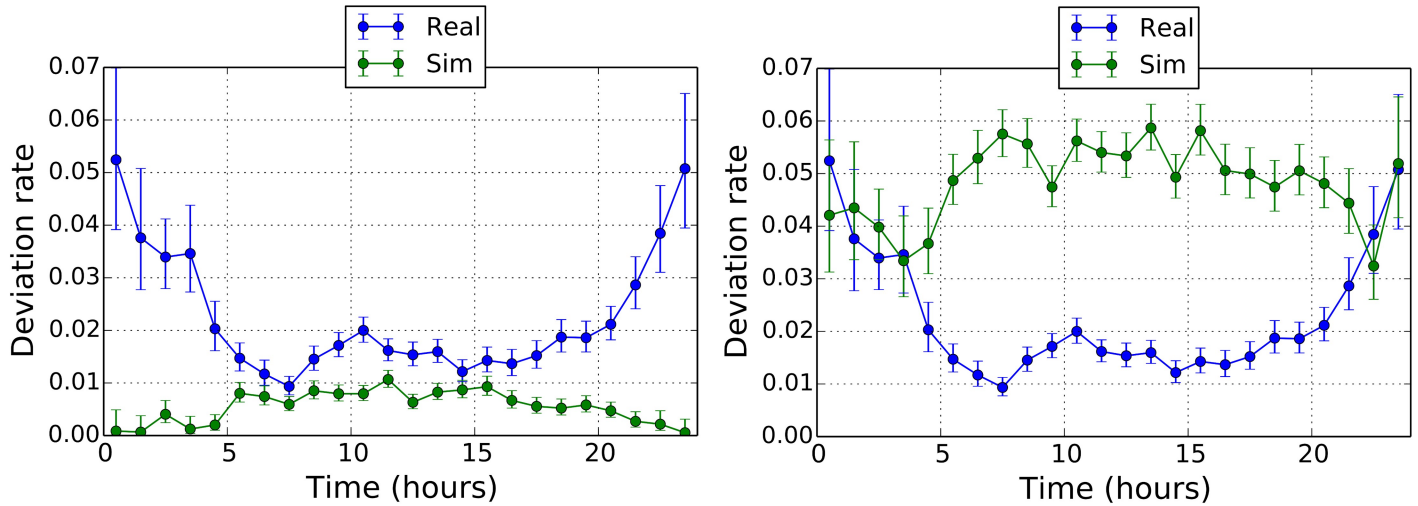


**Fig 6.** Left panel: deviation rates in the “No Directs” case. Right panel: deviation rates in the “No Sector Directs” case.

<https://doi.org/10.1371/journal.pone.0175036.g006>

In Fig 7 we show the fraction of the different decisions taken by controllers. The three decisions controllers can take are (i) issuing a direct, (ii) re-routing a flight trajectory, and (iii) temporarily changing the flight level of a trajectory. We label the total number of operations in a given one hour interval as  $N_O$ .  $N_D$  is the number of directs issued by controllers in the time

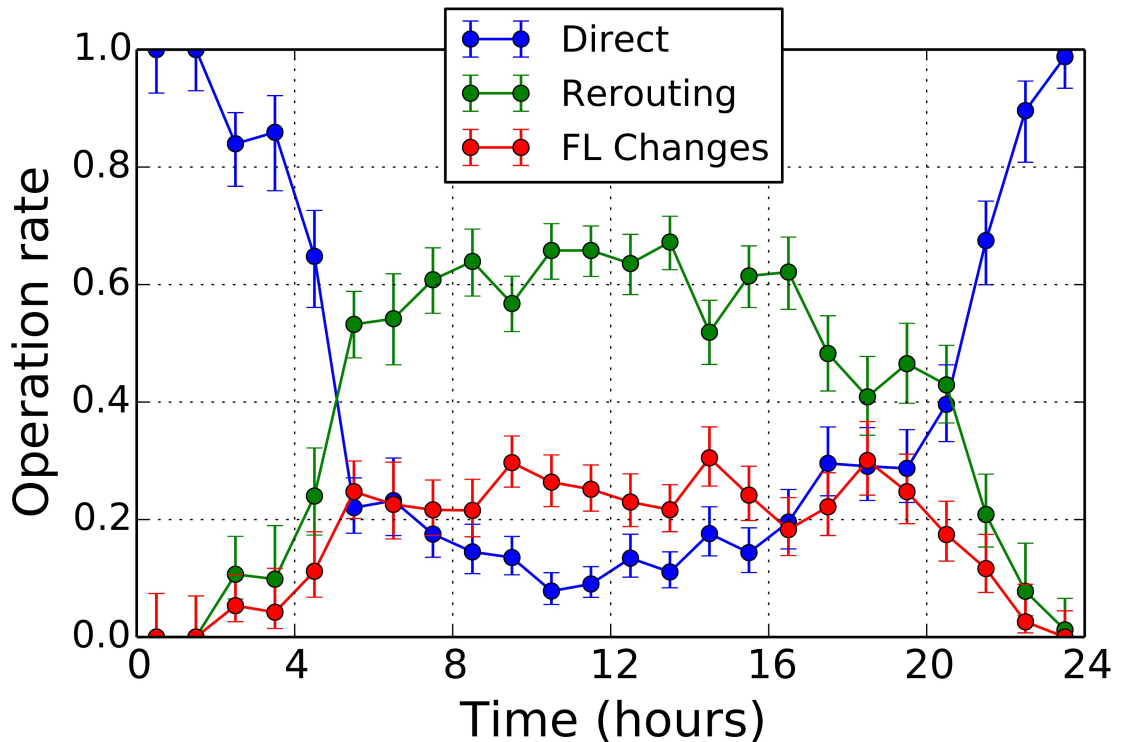


**Fig 7.** Controllers’ operation rate: The ratio  $N_F/N_O$  between the number  $N_F$  of flight level changes (red circles) and the total number of operations  $N_O$ , the ratio  $N_R/N_O$  between the number  $N_R$  of re-routings (green circles) issued to solve possible conflicts and  $N_O$ , the ratio  $N_D/N_O$  between the number  $N_D$  of directs (blue circles) and  $N_O$ , where  $N_O = N_F + N_R + N_D$ . The error bars correspond to the 95% Wilson confidence interval.

<https://doi.org/10.1371/journal.pone.0175036.g007>

interval. Similarly,  $N_R$  is the number of re-routings and  $N_F$  is the number of flight level changes. In Fig 7 we show the ratio of directs  $N_D/N_O$  (blue circles), the ratio of re-routings  $N_R/N_O$  (green circles), and the ratio of flight level changes  $N_F/N_O$  (red circles). The error bar is to the 95% Wilson confidence interval. The ratio of flight level changes (red circles) and the ratio of re-routings (green circles) issued to solve possible conflicts are larger during day-time rather than during night-time. It is worth noting that the number of re-routing is always higher than the number of flight level changes. This is a satisfactory outcome of our model consistent with the feedback we have received from ATM experts. The ratio of directs (blue circles) behaves in the opposite way. This is again expected, given the fact that lower traffic conditions during night allows for the possibility of optimizing trajectories more easily [26]. During day-time, the sector workload can be different for different sectors and therefore maximal sector capacity is not reached at the same time for all sectors. This can be an explanation why directs are also issued during day-time.

### 5.1 Conflict resolution in the ABM

In this section we discuss the ability of our model in performing conflict resolution by investigating the distance observed between all pairs of aircraft flying during a given day.

In Fig 8 we show the cumulated distribution of the distance between any pair of aircraft for a simulation performed for the first day of AIRAC 334. The red curve shows the distribution of the planned trajectories, the blue curve (labeled as simulation I) is the cumulated

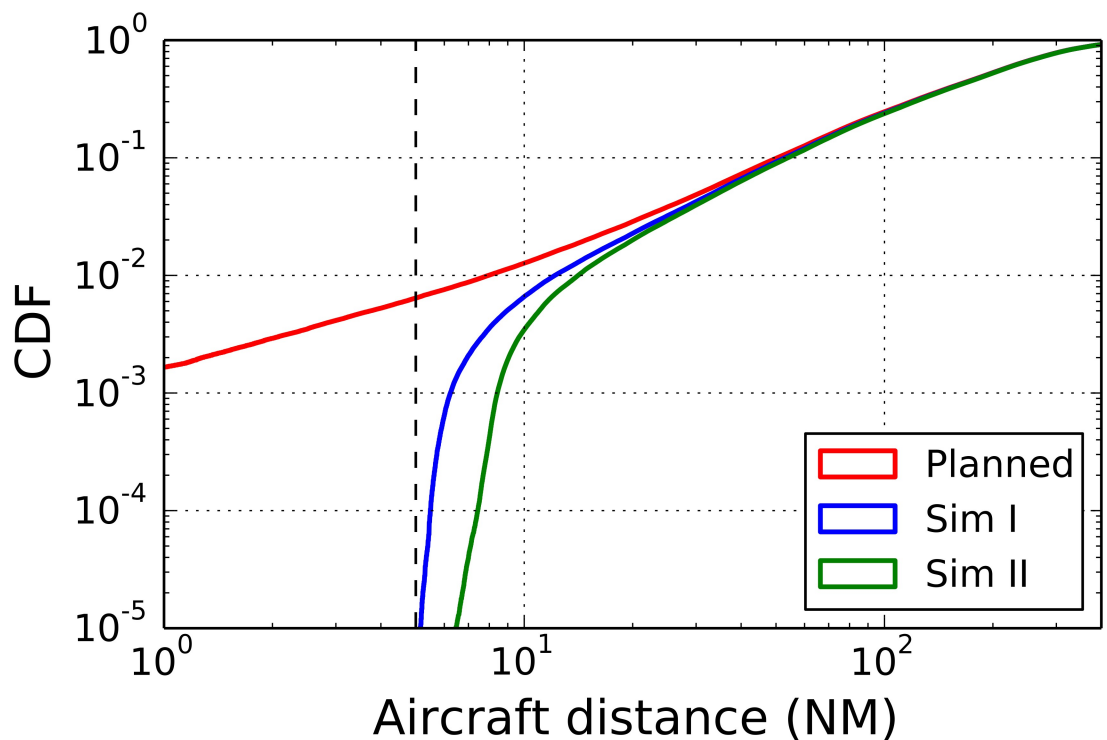


**Fig 8. Cumulative distribution of the distance between any pair of aircraft.** The red curve shows the cumulative distribution of the planned trajectories, the blue curve (simulation I) is the cumulative distribution of flight trajectories simulated with our model by considering a fixed safety threshold of 5 NM. The green curve (simulation II) is the cumulative distribution of flight trajectories simulated with our model when the safety threshold increases with the look-ahead by setting  $\Delta d_{the} = 0.33$ . The cumulative distribution is obtained by considering all flights of AIRAC 334 and the associated simulations.

<https://doi.org/10.1371/journal.pone.0175036.g008>



distribution of the flight trajectories simulated with our model by using the safety threshold of 5 NM. The green curve (labeled as simulation II) is the cumulated distribution of the flight trajectories simulated with our model by using a safety threshold that increases with the look-ahead, as described in section 3.5. Specifically, in the second simulation we set  $\Delta d_{thr} = 0.33$ .

In the figure we highlight as a vertical line the value of 5 NM. It is worth noting that both the blue and the green lines show values that are on the right of the vertical line. This means that our ABM solves all conflicts that were present in the planned flight of the day. The blue line presents values that are quite close to the 5 NM threshold whereas, as expected, the green line has lower values for distances slight above 5NM, thus indicating that aircraft are more separated.

The parameter  $\Delta d_{thr}$  therefore allows the model to fine tuning the probability of observing a pair of aircraft with a given minimal distance in a given day. As also recalled in Table 1,  $\Delta d_{thr}$  is a parameter that might in principle reflect the ATCOs behavior when managing traffic with a large look-ahead. In fact, a large  $\Delta d_{thr}$  would indicate that human controllers tend to be overly safe when managing trajectories with a large look-ahead and tend to separate aircraft pairs more than it is needed. The model shows that this might end up in having aircraft separated more the 5 NM and therefore in a non-optimal usage of the available airspace that in turn leads to a reduction of the maximal sector capacity. On the other hand, a small  $\Delta d_{thr}$  would indicate that human controllers are rather confident about their procedures even for aircraft that are far away. In this case our simulations indicate that all available airspace is used which might lead to an optimal assessment of sector capacity.

### 5.2 Spatial heterogeneity of the operations

In Fig 9 we show the map of navigation points with the information about the type of operations controllers do in their neighboring. In the left panel we show re-routings. In the central panel we show flight level changes, while in the right panel we show directs. In all panels the size of circles is proportional to the number of operations performed. All values refer to the

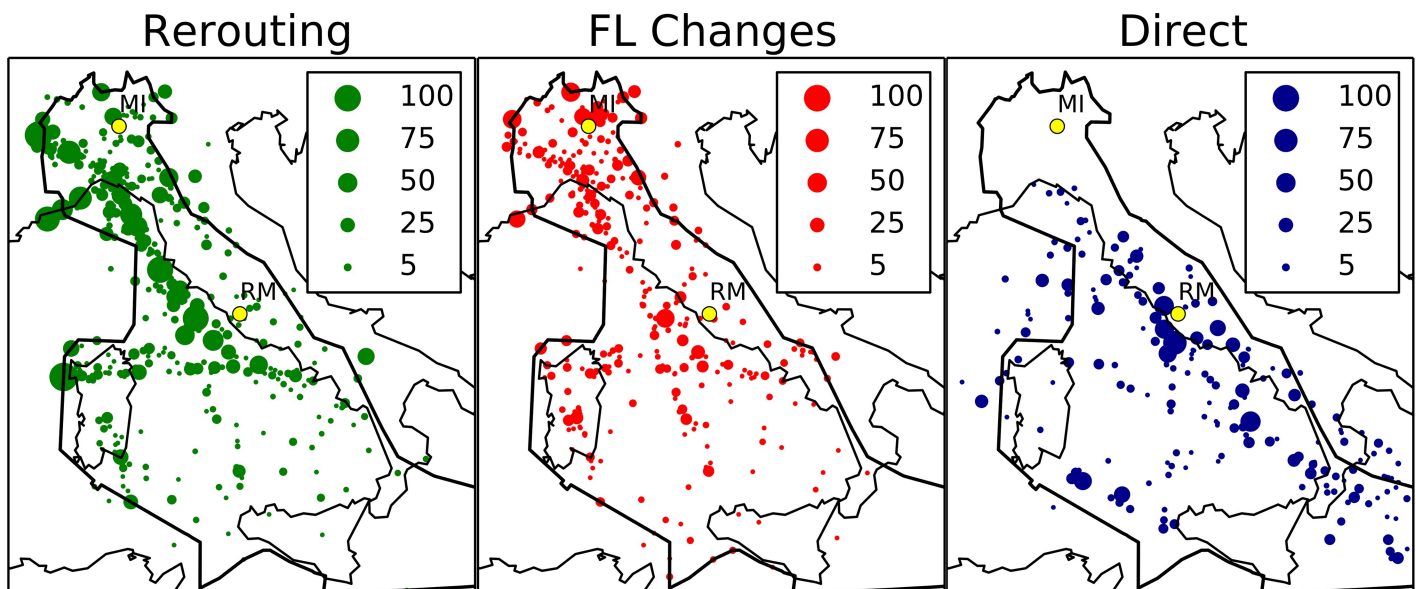


**Fig 9. Map of navigation points with the information about the type of operations controllers have to do in their neighboring.** Left panel (green): the size of each circle is proportional to the number of re-routings. Central panel (red): the size of each circle is proportional to the number of flight level changes. Right panel (blue): the size of each circle is proportional to the number of directs.

<https://doi.org/10.1371/journal.pone.0175036.g009>

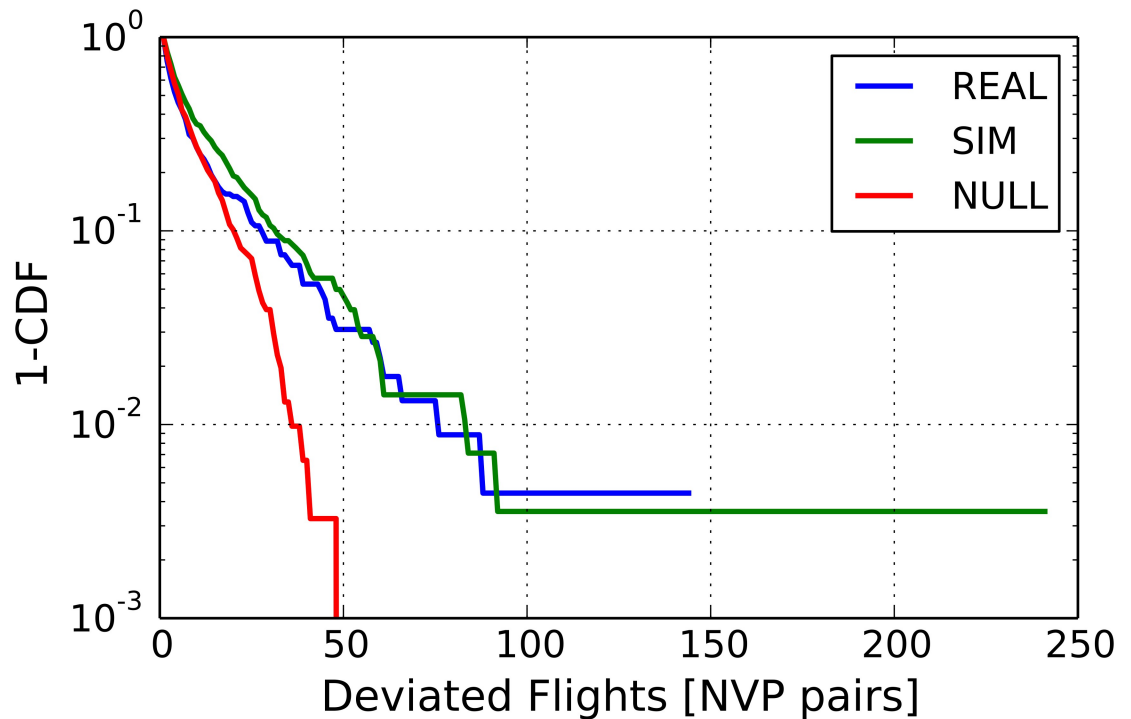


**Fig 10. Complementary cumulative distribution of the difference  $M = M_{pp} - M_{pr}$  between the number of planned flights that should have passed through a certain trajectory segment  $M_{pp}$  and the number of these flights that actually passed through that trajectory segment  $M_{pr}$ .** The blue line refers to empirical data, while the green curve refers to data obtained through numerical simulations of our ABM. The red curve refers to data obtained by performing a random sampling of the missed flight in each trajectory segment.

<https://doi.org/10.1371/journal.pone.0175036.g010>

334 AIRAC. Interestingly, the navigation points with the highest number of re-routings are aligned along the route between Milan and Rome, which shows the highest traffic levels, as indicated in Fig 9. On the other hand the highest number of directs is issued either in central Italy (most probably in proximity of Fiumicino airport) or in the Tyrrhenian Sea, between Naples and Sicily, where traffic levels are less pronounced than in the northern region, as indicated in Fig 9. The location of flight level change operations highlights those navigation points where controllers have difficulties in solving conflicts and use flight level change as the last resort for conflict solution.

According to the controllers of the LIRR ACC interviewed within the ELSA research project a similar result also holds for operations performed by real ATCOs. Indeed, the ATCO operations do not uniformly affect the flux of aircraft in the airspace. Rather, ATCOs typically concentrate their operations on specific segments of flight trajectories (i.e. on the path joining two neighboring navigation points). This is clearly shown by the results summarized in Fig 10. In this figure we show the distribution of the difference  $M = M_{pp} - M_{pr}$ . Here  $M_{pp}$  is the number of planned flights that should have passed through a certain trajectory segment and  $M_{pr}$  is the number of these flights that actually passed through that trajectory segment. The blue line shows empirical data, while the green line refers to data obtained through numerical simulations of our ABM. The red line refers to a random allocation of  $M$  values relative to the missed flight in each trajectory segment. This random allocation preserves (i) the planned number of flights in each trajectory segment  $M_{pp}$  and (ii) the sum  $\sum_{link} M$  for the whole ACC. Such random sampling therefore preserves the planned heterogeneity of the system as well as the global number of operations done by the controllers.

Two comments are in order. On one hand, one can notice that the ABM well reproduces the empirical observations. On the other hand, it is worth noticing that these two distributions show tails that are fatter than those of the distribution obtained with the random sampling. This indicates that there are trajectory segments where the number of operations done by the controllers is higher than what should be expected by the random null model. This clearly suggests that ATCO operations tend to be focused on specific regions of the ACC. The comparison with such simple random null model therefore allows us to highlight the presence of specific regions in the airspace that cannot be explained just with the heterogeneity of the flux of aircraft: it is therefore a genuine effect produced by the ATCOs and it is quite well reproduced by the ABM.

However, although the ABM well reproduces the existence of regional heterogeneity, it is worth emphasizing that there are airspace regions where the ABM and human ATCOs manage traffic in a different way. In Fig 11 we show the difference  $M$  in a specific region of the ACC located close to Genoa and characterized by high traffic conditions. The left panel refers to the empirical case while the right panel refers to numerical simulations performed with our ABM. The difference  $M$  is here shown through a color scale reported on the right of each panel. One can see that there are trajectory segments where ATCOs do not modify planned trajectories (lighter colors) that are instead quite heavily affected by the ABM (darker colors) and viceversa.

In fact, this should not be surprising given the fact that ATCOs have to deal with tactical conditions (weather events, aircraft problems, . . .) that our ABM does not take into account. Moreover, this different behavior might also be due to the fact that human controllers tend to be overly safe and therefore have a conservative style in managing the aircraft trajectories.

### 6 Dependence of directs and conflict resolution rates from model parameters

Finally, we report on how our model performs under parameters different from the ones chosen for calibration. Specifically, we evaluate the performances of our model with respect to

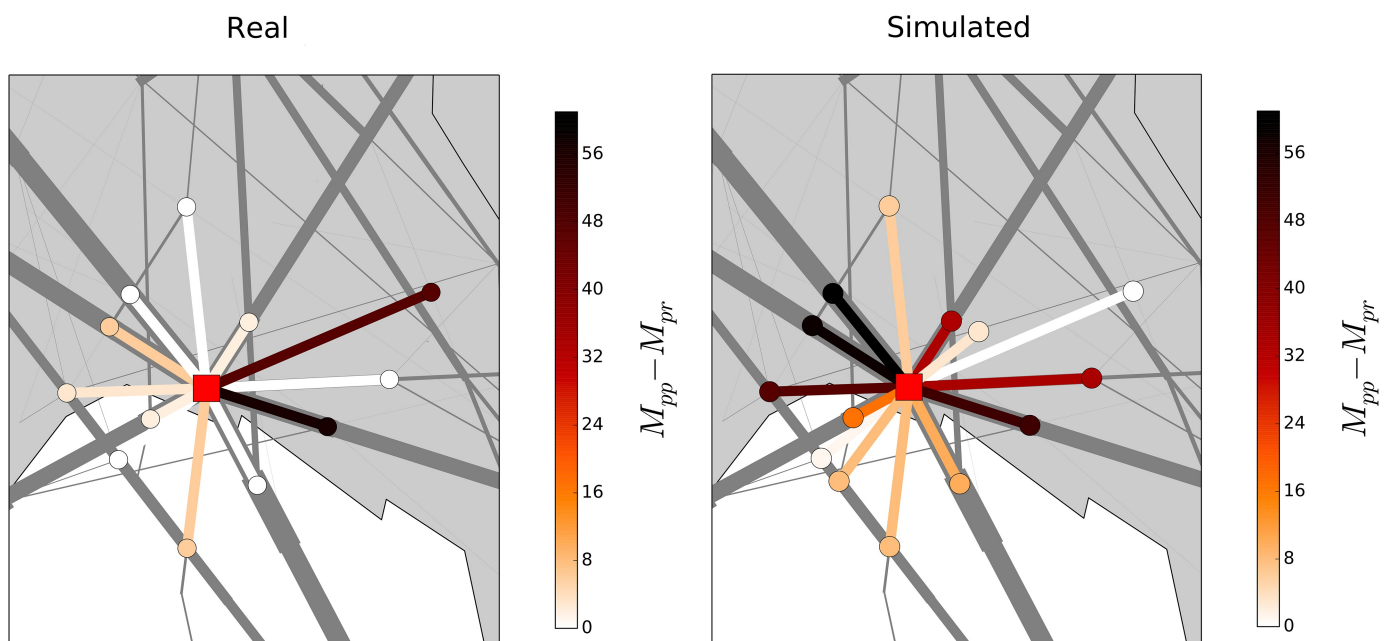


**Fig 11. Difference  $M$  in a specific region of the ACC located close to Genoa, Italy.** The left panel refers to the empirical case while the right panel refers to numerical simulations performed with our ABM. The difference  $M$  is here shown through the color-code reported on the right of each panel.

<https://doi.org/10.1371/journal.pone.0175036.g011>

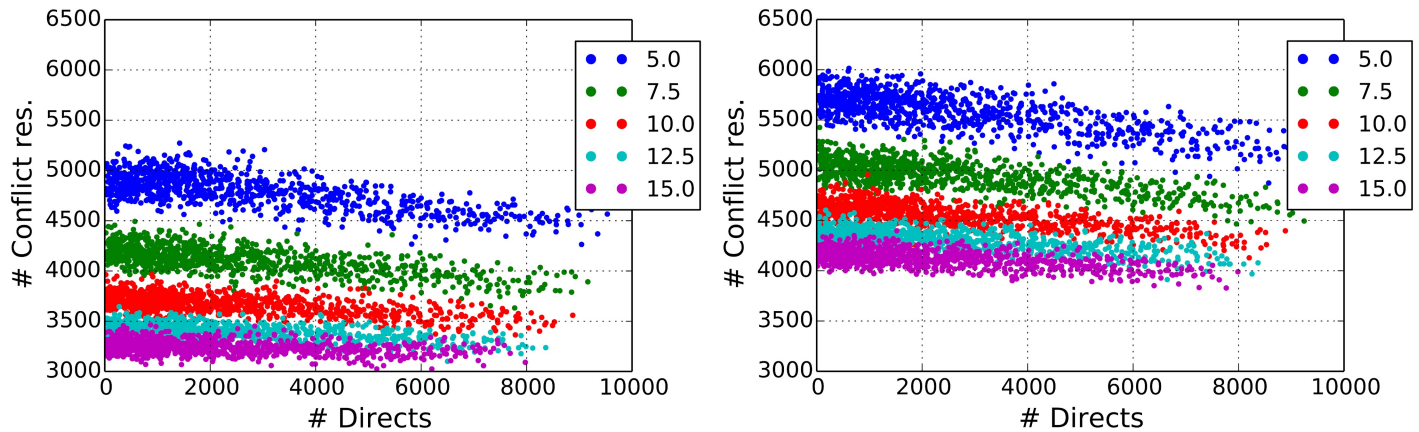


**Fig 12. Number of conflict resolutions as a function of the number of issued directs.** Each point in the plot corresponds to the result of a simulation of the ABM performed with a pair  $(p_d, x_c)$  of parameters selected in the range  $p_d \in [0.03, 0.5]$  (with step of 0.01567),  $x_c \in [0.34, 1.5]$  (with step of 0.03867). Different colors refers to different values of the look-ahead  $\Delta t_l$ . In all simulations  $\Delta t_d = 15$  min. The simulations on the left panel are made with a perfect forecast. The simulations on the left panel are done by introducing a noise in the velocity of aircraft ( $l_v = 0.1$ ). This noise strongly affects the reliability of forecast of flight trajectories.

<https://doi.org/10.1371/journal.pone.0175036.g012>

model decisions concerning directs and conflict resolutions as a function of procedures followed by air traffic controllers and air traffic conditions of sectors.

Results of our investigation are summarized in Fig 12. In the left panel of Fig 12 we show the number of actions that the controllers perform in order to solve conflicts, i.e. re-routings and flight level changes, as a function of the number of directs for the five values of  $\Delta t_l$  shown in the legend. Each point in the plot corresponds to the result of a simulation of the ABM performed with a pair  $(p_d, x_c)$  of parameters selected in the range  $p_d \in [0.03, 0.5]$  (with step of 0.01567),  $x_c \in [0.34, 1.5]$  (with step of 0.03867). The figure suggests the existence of a linear negative relation between the number of operations needed to solve conflicts and the number of directs, thus indicating that the number of unsolved conflicts decreases when the number of directs issued increases.

These results refer to ATCOs able to do a perfect forecast within the look-ahead  $\Delta t_d$  used when directs are issued. In reality, many unexpected factors can contribute to make uncertain a forecast. Uncertainty can result for example from a flight entering the airspace within  $\Delta t_d$  unexpectedly or a weather event, or some errors in the forecast of aircraft positions. We evaluate the performance of our ABM model with respect to this type of uncertainty by performing a series of simulations in the presence of a source of noise. Specifically, the source of noise is introduced in the velocity of aircraft. In the right panel of Fig 12 we show the results of a numerical simulation obtained by introducing noise in the velocity estimation of the aircraft. The parameter used is  $l_v = 0.1$  which is a quite large value. This produces the effect of increasing the number of needed conflict resolutions especially for simulations with a high value of the look-ahead.

In Table 2 we report the result of a linear fitting procedure on the five sets of simulations obtained for different values of  $\Delta t_l$  and shown in Fig 12 as points of different colors. The upper part of the table refers to simulations with perfect forecast whereas the lower part refers to simulations in the presence of noise. The  $p$ -value reported in a column is the two-sided  $p$ -value of the null hypothesis that the slope of the linear relationship is zero. Indeed, the low  $p$ -values observed support the existence of a linear relationship between directs and conflict resolution events, although the slope value can be quite small in all considered cases. In fact, the correlation values reported in the fourth column are indicating a statistically robust negative relationship between directs and conflict resolution events.

**Table 2. Summary statistics of the result of a linear fitting procedure on the five sets of simulations obtained with different values of  $\Delta t_i$ .** Other parameters are changed as described in the text. The upper part of the table refers to simulations with perfect forecast whereas the lower part refers to simulations in the presence of noise. The simulations in the presence of noise are obtained by setting  $l_e = 0.1$ .

lookahed (min)	noise	slope	intercept	correlation coef.	p-value	std err
5.00	0.0	-0.052	4939	-0.691	$10^{-128}$	0.002
7.50	0.0	-0.040	4215	-0.653	$10^{-110}$	0.002
10.0	0.0	-0.028	3734	-0.571	$10^{-79}$	0.001
12.5	0.0	-0.021	3444	-0.522	$10^{-64}$	0.001
15.0	0.0	-0.013	3273	-0.342	$10^{-26}$	0.001
5.00	0.1	-0.060	5749	-0.719	$10^{-144}$	0.002
7.50	0.1	-0.046	5073	-0.694	$10^{-130}$	0.002
10.0	0.1	-0.039	4650	-0.685	$10^{-125}$	0.001
12.5	0.1	-0.030	4370	-0.582	$10^{-82}$	0.001
15.0	0.1	-0.027	4186	-0.555	$10^{-74}$	0.001

<https://doi.org/10.1371/journal.pone.0175036.t002>

It is worth noting that slopes observed in the presence of noise are systematically higher in absolute value than in the case of perfect forecast. This seems to suggest that also in the presence of enhanced uncertainty issuing directs reduces the number of conflicts to be resolved.

## 7 Conclusions

In this work we have presented an agent-based model of the ATM system that aims at modeling the interactions between aircraft and air traffic controllers at a tactical level. We have presented in detail the different modules of the model whose core is given by the conflict detection and resolution module of section 3.5 and by the directs module of section 3.7.

In section 4 we have given an example of the calibration of our model done in order to obtain simulations describing the statistical regularities about the rate of flight trajectory deviations observed in empirical data.

In section 5 we have reported results obtained with our model. First, we explicitly show that the calibrated model is able to reproduce the existence of regional localization of ATM operations, i.e. the fact that ATCO operations tend to be focused on specific points of the ACC. Finally, we have shown scenario simulation results about the relationship between directs and conflict resolution events conditioned to model parameters.

Our model can be used to give useful insights about the functioning of the ATM system. We are aware that our model is very basic. For example, our basic agent based model does not implement any learning mechanism as done for example in other models [8] or specific fitness measures besides the fact that in the conflict resolution module we must consider the shortest trajectory amongst the possible ones. Furthermore, the model implements a local resolution of conflicts according to a priority list randomly ordered. The way our model solves conflicts is fast from a computational point of view but provides solutions that are not optimized at a global level. In fact, our ABM does not take into account all flight trajectories simultaneously in order to solve potential conflicts. This characteristic of our approach implies that our ABM checks potential conflicts of a flight trajectory several times during its flight across the ACC. We are fully aware of this limitation of our model. We implemented such a solution because we wanted to develop an ABM mimicking the way air traffic controllers work in reality.

Indeed, we believe that such solution might be quite effective in the SESAR scenario simulations. In fact, we might simulate a scenario where controllers have a role less preeminent than in the current scenario and some basic conflict-resolution actions are left to the single aircraft. In this respect, our model might mimic a scenario where pilots, that clearly have not a global

vision of the system, endowed with a set of policy rules assigned by their airlines, will perform an *active* conflict resolution at a tactical level, thus realizing a sort of self-organization amongst aircraft. Along similar lines, other possible ways for further research starting from the present model regard the possibility of augmenting our model capabilities by implementing learning and self-adaptation mechanisms as well as some level of intelligence for the agents.

## Acknowledgments

This work was co-financed by EUROCONTROL on behalf of the SESAR Joint Undertaking in the context of SESAR Work Package E—ELSA research project. We thank the Deep Blue Srl team for providing us useful insights about the ATM system. We also thank all past participants to the ELSA project for interesting discussions.

## Author Contributions

**Conceptualization:** CB SM RNM.

**Data curation:** CB SM.

**Formal analysis:** CB SM RNM.

**Funding acquisition:** SM RNM.

**Investigation:** CB.

**Methodology:** CB SM RNM.

**Project administration:** SM RNM.

**Software:** CB.

**Supervision:** SM RNM.

**Validation:** CB SM RNM.

**Visualization:** CB.

**Writing – original draft:** CB SM RNM.

**Writing – review & editing:** CB SM RNM.

## References

1. SESAR (2007), “SESAR Concept of Operations” [https://www.eurocontrol.int/sites/default/files/field\\_tabs/content/documents/sesar/20070717-sesar-conops.eps](https://www.eurocontrol.int/sites/default/files/field_tabs/content/documents/sesar/20070717-sesar-conops.eps); SESAR (2012), “SESAR Concept of Operations Step 1” [http://www.sesarju.eu/sites/default/files/documents/highlight/SESAR\\_ConOps\\_Document\\_Step\\_1.eps](http://www.sesarju.eu/sites/default/files/documents/highlight/SESAR_ConOps_Document_Step_1.eps).
2. EU Commission (2010) “Commission regulation (EU) no 691/2010”.
3. EUROCONTROL (2005), “Final report on european commissions mandate to support the establishment of functional airspace blocks (fabs)”. EUROCONTROL (2012), “Free Route Developments in Europe”.
4. Cook A.C., Rivas D. Eds. (2016) “Complexity Science in Air Traffic Management” (Routledge, England, 2016)
5. Heath B., Hill R., Ciarallo F. (2009) “A survey of agent-based modeling practices (January 1998 to July 2008)”, *Journal of Artificial Societies and Social Simulation*, 12 (4), 9–xx.
6. Windrum P., Fagiolo G., Moneta A. (2007) “Empirical validation of agent-based models: Alternatives and prospects”, *Journal of Artificial Societies and Social Simulation*, 10 (2), 8–xx.

7. Kuchar J. K., Yang L. C. (2000) "A Review of Conflict Detection and Resolution Modeling Methods", *IEEE Transactions on Intelligent Transportation Systems*, 1 (4), 179–189. <https://doi.org/10.1109/6979.898217>
8. Agogino A. K., Tumer K. (2012) "A multiagent approach to managing air traffic flow", *Auton Agent Multi-Agent Syst*, 24, 1–25. <https://doi.org/10.1007/s10458-010-9142-5>
9. Shah A. P., Prichett A. R., Feigh K. M., Kalaver S. A. (2005) "Analyzing air traffic management systems using agent based modeling and simulation", *Proceedings of the 6th USA/Europe Seminar on Air Traffic Management Research and Development*. (Baltimore, 27-30 June 2005, USA).
10. Durand N., Alliot J.-M. (1997) "Optimal Resolution of En-Route Conflicts", *Proceedings of the 1st USA/Europe Seminar*. (Saclay, 17-19 June 1997, France).
11. Bilimoria K.D. (2000) "A geometric optimization approach to aircraft conflict resolution", *Proceedings of the AIAA guidance, navigation, and control conference and exhibit*. (Reston, 14-17 August 2000, USA).
12. Eby M. S., Kelly W. E. (1999) "Free Flight Separation Assurance Using Distributed Algorithms", *Proceedings of the IEEE Aerospace Conference*, Vol. 2, pp. 429-441. (Snowmass at Aspen, 06-13 March 1999, USA).
13. Bongiorno C., Miccichè S., Mantegna, R. N., Gurtner G., Lillo F., Valori L., Ducci M., Monechi B., Pozzi S. (2013) "An Agent Based Model of Air Traffic Management", *Proceedings of The Third SESAR Innovation Days EUROCONTROL*. (Stockholm, 26-28 November 2013, Sweden).
14. Monechi B., Servedio V. D. P., Loreto V. (2014) "An Air Traffic Control Model Based Local Optimization over the Airways Network", *Proceedings of The Fourth SESAR Innovation Days EUROCONTROL*. (Madrid, 25-27 November 2014, Spain).
15. Monechi B., Servedio V. D. P., Loreto V. (2015) "Congestion Transition in Air Traffic Networks", *PLoS ONE* 10(5), e0125546. (2015). <https://doi.org/10.1371/journal.pone.0125546> PMID: 25993476
16. Bongiorno C., Miccichè S., Ducci M., Gurtner G., (2015) "ELSA Air Traffic Simulator: an Empirically grounded Agent Based Model for the SESAR scenario", *Proceedings of The Fifth SESAR Innovation Days EUROCONTROL*. (Bologna, 3-5 December 2015, Italy).
17. Bongiorno C., Gurtner G., Ducci M., Miccichè S. (2017) "An Empirically grounded Agent Based simulator for the Air Traffic Management in the SESAR scenario", *JATM*, accepted for publication, (2017).
18. [http://www.eurocontrol.int/eec/public/standard\\_page/NCD\\_nevac\\_home.html](http://www.eurocontrol.int/eec/public/standard_page/NCD_nevac_home.html)
19. Lillo F., Miccichè S., Mantegna R.N., Beato V., Pozzi S. (2011) "Elsa project: Toward a complex network approach to atm delays analysis", *Proceedings of the SESAR Innovation Days EUROCONTROL*. (Toulouse, November 2011, France).
20. Gurtner G., Valori L., Lillo F. (2015) "Competitive allocation of resources on a network: an agent-based model of air companies competing for the best routes", *JSTAT* 2015(5), P05028. <https://doi.org/10.1088/1742-5468/2015/05/P05028>
21. Kernighan B. W., Ritchie D. M. (1988) "The C Programming Language", (Prentice Hall, England, 1988).
22. Smart W. M. (1960) "Text-Book on Spherical Astronomy", (Cambridge University Press, England, 1960, 6th ed.).
23. International Civil Aviation Organization (ICAO), Document n. 4444 "Procedures for Air navigation Services—Air Traffic Management", 15<sup>th</sup> edition, (2007), available at: <http://code7700.com/pdfs/icaodoc444415thedition.pdf>
24. ELSA project, "E.02.18-ELSA D1.3 Statistical Regularities in ATM—final draft", Version: 21/12/2012, (Restricted audience)
25. ELSA project description: <http://complexworld.eu/wiki/ELSA>
26. Bongiorno C., Miccichè S., Mantegna R. N., Gurtner G., Lillo F. (2016) "Statistical characterization of deviations from planned flight trajectories in air traffic management", *JATM* 58, 152D163 (2017).
27. Wilson E.B. (1927) "Probable inference, the law of succession, and statistical inference", *Journal of the American Statistical Association* 22, 209–212. <https://doi.org/10.1080/01621459.1927.10502953>